RECORDING THE SEISMIC SIGNAL GENERATED BY HYPERVELOCITY IMPACT IN EXPERIMENTS AND NUMERICAL MODELS. N. Güldemeister[1], D. Moser[2], K. Wünnemann[1] and C. Grosse[2], [1]Museum für Naturkunde, Leibniz Institute for Research on Evolution and Biodiversity, Invalidenstrasse 43, 10115 Berlin, Germany (nicole.gueldemeister@mfn-berlin.de), [2]Technische Universität München, Non-destructive Testing Laboratory, München, Germany.

Introduction: Meteorite impacts cause a series of environmental consequences, one of which is the generation of ground motions that may exceed the magnitude of the largest earthquakes [1,2]. Impacts generate shock waves that attenuate with distance until they eventually turn into seismic waves. Although shock wave decay has been studied in much detail and is well parameterized the seismic energy induced by meteorite impact is only poorly known. Seismic signals have been recorded in explosion experiments [3] and in hydrocode models of the formation of the Chicxulub crater [4]. The so-called seismic efficiency k relates the seismic energy E_{seis} with the kinetic energy E_{kin} of the impactor ($E_{seis}= k\ E_{kin}$) and is usually estimated to range between 10^{-3} and 10^{-5} [5].

In the framework of the "MEMIN" (multidisciplinary experimental and modeling impact crater research network) project a suite of hypervelocity impact experiments with sandstone, tuff, and quartzite targets on a decimeter scale have been carried out [6]. We use acoustic emission (AE) techniques in high spatiotemporal resolution and numerical modeling to determine the characteristic of elastic waves arriving at varying distances on the laboratory scale. In a second step these data may be used to quantify the seismic efficiency of hypervelocity impacts. The acoustic emission techniques can be considered to be a form of microseismicity that is similar to earthquakes generated during the failure process. We consider a nonporous quartzite and a porous sandstone target as the presence of porosity is expected to affect wave propagation significantly. Here we present preliminary results to validate our numerical models against the recorded seismic signals in the experiments. In particular we focus on the propagation speed of the seismic signals. A direct comparison of the amplitude of the waves in experiment and numerical model requires thorough calibration of the AE transducers, first.

Methods: The acoustic emission technique uses AE transducers attached to the surface as seen in Fig. 1a with which the elastic waves generated during an impact can be recorded and analyzed with respect to their origin (impact point) [5]. In the experiment the arrival time of the first wave signal is recorded at different distances to the point of impact to determine the propagation velocities. Additionally, we used methods such as ultrasound tomography (US), microcomputer tomography or modal analysis to characterize the elastic properties (elastic modulus, p-wave velocity) of the target before and after the impact. For the numerical models we used the multi-material, multi-rheology hydrocode iSALE [e.g. 6,7,8] coupled with the ANEOS [9] for quartzite [10] to describe the thermodynamic behavior of the material. For sandstone the ANEOS has been combined with the ε-α compaction model [6] to simulate porous material [11]. The model setup (Fig. 1b) and material properties have been calibrated in a previous study in much detail [11]. In contrast to the experiments where the target is a rectangular block we assumed a cylindrically symmetric geometry of the target in the numerical models. Accordingly, the location of the sensors had to deviate from their actual location in the experiments keeping the distance to the point of impact the same. We recorded different thermodynamic and mechanical parameters as a function of time and picked the arrival time of the first detectable signal. As the wave velocity depends on porosity, which changes dynamically due to shock-induced crushing of open pores space, it was necessary to modify the material model. The new model considers a wave velocity for nonporous quartzite of 5000 m/s and for porous sandstone (25% porosity) of 2900 m/s obtained by US measurement. For intermediate porosities (0-25%) as a result of different degree of shock wave compaction we assume a linear dependency of wave velocity on porosity.

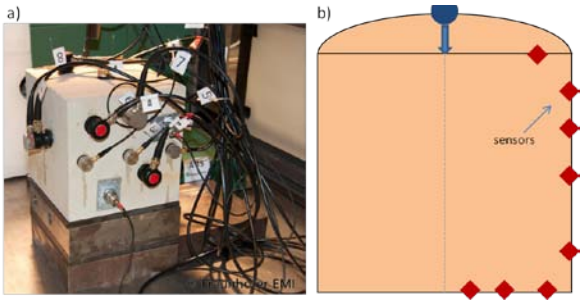

Fig. 1: a) Setup of sensors and sandstone target for the acoustic emission experiment**. b)** Numerical setup of the target block with sensors.

Results: First-arrival-times of impact-induced waves picked from time-series recorded at experiments and numerical models with a quartzite and a sandstone target are plotted versus distance in Fig.2. The time series are shown in Fig. 3. From the slope of a line fitted to the experimental and the modeling data we obtained a wave velocity of about 5000 m/s for the quartzite targets (Fig. 2). This velocity corresponds to the input

parameter for the speed of sound, as it should be. For the sandstone target the velocity determined from the first-arrival-times in the experiment is 3200 m/s and deviates from the numerical model where we find a velocity of 3900 m/s (Fig.2). Both results are in excess of the US velocity measured before the experiment of 2900 m/s. Note, the velocity determined from first-arrival-times has to be larger than the US-velocity as the wave travels initially at the speed of a shock wave which is larger than the speed of sound. A detailed comparison of the numerical and experimental time series for quartzite and sandstone is shown in Fig. 3. Generally, we find a good agreement at different sensors between numerical models and experimental data in terms of the arrival time and signal phase (compressive wave is indicated by a negative amplitude). Note, the experimental data have been capped due to overdriving.

Discussion: We demonstrate that it is possible to record the AE in hypervelocity impact experiments and use the data to validate numerical models. At the current state we are only able to reproduce first-arrival-times in nonporous quartzite. In porous material the elastic properties change dynamically as porosity is crushed out by shock compression. We account for this effect by including a linear dependency of the speed of sound on porosity. As a result we find a significantly reduced propagation velocity of the elastic wave that is still approx. 20% above the velocity measured in the experiments. Further improvements of our material model are required in particular for the behavior of porous material before our approach allows for better quantifying the seismic efficiency of meteorite impact.

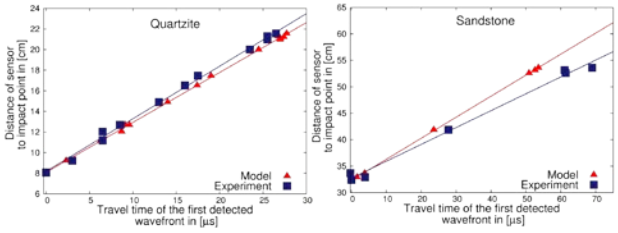

Fig. 2: Linear propagation of the first wave front inside the target for the experiment and the model. The plot shows the distances of different sensors versus first arrival time. The average wave velocity is measured to be around 5090 m/s (experiment) and 4900 m/s (model) for quartzite (**left**) and 3200 m/sec (experiment) and 3980m/s (model) for sandstone (**right**).

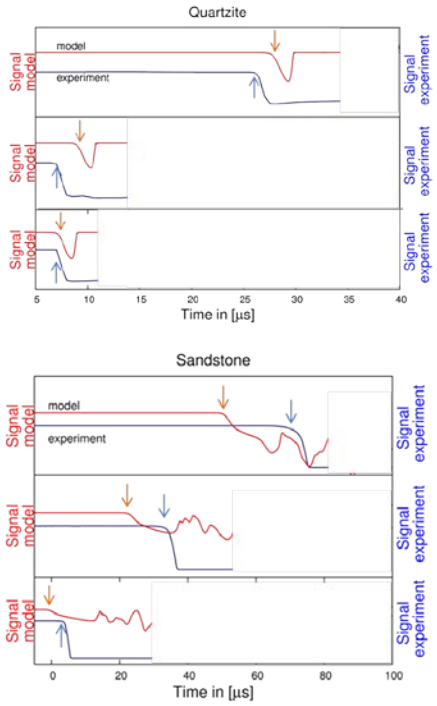

Fig. 3: Comparison of numerical and acoustic emission signals of the first detectable wave signal recorded by three sensors of different distances to the impact point for quartzite (top) and sandstone (bottom). The distances of the sensors to the impact point increase from bottom to top. The arrows represent the point in time when the first detectable signal has been picked. Note the different scale on the x axis and that the AE signal has been capped.

Acknowledgment: This work was funded by DFG grant WU 355/6-1.

References: [1] Collins G. S. et al. (2005) *MAPS*, 40, 817-840. [2] Toon, O.B., et al. (1997), *Rev. Geophys*., 35, 1, 41–78. [3] Schultz, P.H. & Gault, D.E. (1974), Seismic effects from major basin formations on the Moon and Mercury, Earth, Moon Planets, 12, 2, 159–177. [4] Ivanov B.A. (2004) *Sol. Sys. Res.,* 39,381-409. [5] Melosh H.J. (1989), Impact Cratering, Oxford Univ. Press, New York, p. 245. [6] Kenkmann T. et al. (2011) *MAPS,* 46, 875-889. [5] Grosse C. and Ohtsu M. (2008) Springer publ., *page 400 pp*. [6] Wünnemann K. et. al. (2006) *Icarus,* 180, 514-527. [7] Ivanov, B. A., et al. (1997), *Int. J. Imp. Eng.* 20, 411-430. [8] Amsden A. A. Et al. (1980) *LA-8095 Report*, Los Alamos National Lab., 101 p. [9] Thompson S. L and Lauson H. S. (1972), SC-RR-71 0714, 119pp. [10] Melosh H. J. (2007) *MAPS*, 42, 2079-2098. [11] Güldemeister N. et al. (2012) *MAPS,* 47, in press.